

Yongmei Zhou* and Roland Stull
University of British Columbia, Vancouver, BC, Canada

Robert Nissen
Environment Canada, Vancouver, BC, Canada

1. INTRODUCTION

The approach of Laroche and Zawadzki (1994, hereafter LZ) is adopted to retrieve the three-dimensional wind field from single-Doppler radar observations of reflectivity and radial velocity over complex terrain. This LZ approach uses the continuity equation as a strong constraint, and the conservation equation for reflectivity as a weak constraint. The control variables are the two horizontal wind components and the lower boundary conditions of w . Because of its simple constraining model and few control variables, LZ is computationally efficient. To reach the desired minimum of the cost function, a scaling guess procedure is used to perform the retrieval from coarse to fine resolution.

2. DESCRIPTION OF THE TECHNIQUE

2.1 Two-step Filter (Tabary and Scialom 2001)

Let (x_i, y_j, z_k) be the Cartesian coordinate of a grid point, and (x_q, y_q, z_q) be the location of measurement q . The first step, applying a Cressman filter, can be expressed as

$$d^2 = \frac{(x_q - x_i)^2}{R_H^2} + \frac{(y_q - y_j)^2}{R_H^2} + \frac{(z_q - z_k)^2}{R_V^2} \quad (1)$$

$$\omega_q^{i,j,k} = \begin{cases} \frac{1 - d^2}{1 + d^2} & d^2 \leq 1 \\ 0 & d^2 \geq 1 \end{cases}$$

which define the ellipsoid of influence around each grid point.

The second step, applying an angular filter, takes into account the angular variations of the unit-viewing vector inside each ellipsoid of influence. The filter weight is given by

$$\omega_q^{i,j,k} = \frac{1}{1 + \frac{\cos^2 \theta}{\cos^2 \theta_0}} \quad (2)$$

Here θ is the angle between the unit-viewing vector at the measurement and the unit-viewing vector at the grid point, and θ_0 is the cutoff angle of the angular filter.

The total weight for each measurement q to a grid point is calculated by the product of weight component $\omega_q^{i,j,k} \omega_q^{i,j,k}$.

2.2 Variational Formalisms

In the LZ approach, two model equations are used as physical constraints. The first, an anelastic form of the continuity equation, is expressed as

$$\frac{\partial u}{\partial x} + \frac{\partial v}{\partial y} + \frac{\partial w}{\partial z} = kw \quad (3)$$

Here u, v and w stand for the eastward, northward, and upward wind component along the x, y and z directions, respectively. The parameter $k = 10^{-4} \text{ m}^{-1}$ for a standard atmosphere.

The second, a conservation equation for reflectivity, is given by

$$\frac{\partial \rho}{\partial t} + \frac{\partial(u\rho)}{\partial x} + \frac{\partial(v\rho)}{\partial y} + \frac{\partial((w + V_T)\rho)}{\partial z} = S \quad (4)$$

* Corresponding author address: Yongmei Zhou, Univ. of British Columbia, Dept. of Earth & Ocean Sciences, Vancouver, BC; email: yzhou@eos.ubc.ca

Here t is time, $\hat{\rho}$ is the radar-observed reflectivity, and S is the source-sink term. V_T is the terminal fall velocity of precipitation particle and can be estimated empirically from the reflectivity data.

LZ uses equation (3) as a strong constraint and equation (4) as a weak constraint. The resulting cost function is given by

$$J = \sum_{n=0}^N [V_{rn} \ \hat{\rho}_{rn}]^T W_v [V_{rn} \ \hat{\rho}_{rn}] + \sum_{n=1}^N \frac{d\hat{\rho}_n}{dt} S^T W_\rho \frac{d\hat{\rho}_n}{dt} S + J_s \quad (5)$$

The vectors V_{rn} and $\hat{\rho}_n$ represent radial velocity and reflectivity values in space at time step n , N is the number of time steps in the analysis, and the tilde represents observed values. W_v and W_ρ are weighting matrices, and the T superscript indicates the transpose of the bracketed matrix.

In order to achieve a more realistic solution, smoothing constraint terms J_s for the horizontal wind components are added to the rhs of equation (5). The smoothing constraint helps eliminate multiple minima in the cost function.

2.3 Scaling Guess Procedure

A scaling guess procedure performs the retrieval from the largest scale to a finer scale. First, a uniform wind at each level is found with a first guess set to zero. In this case, the control variables are u , v , and w over the coarsest domain. Then, these uniform wind values are used as a first guess to retrieve the wind field over a finer domain. The control variables are u , v and the lower boundary conditions of w .

3. APPLICATION TO REAL DATA

Aldergrove Radar is located in the vicinity of Vancouver, British Columbia, Canada. (Lat. 49.0161°N, Lon. 122.4878°W, Elev. 114m). It provides reflectivity and radial velocity data at 0.5°, 1.5° and 3.5° elevation angles with a 10 min cycle. The range resolution is 500 m and azimuth resolution is 0.5°. The maximum range is 112 km. Mountains caused some blockage of scans near the radar site (Fig. 1)

3.1 Dataset Description

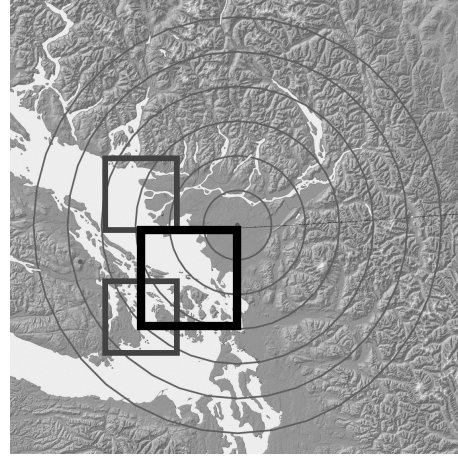


Fig. 1 The background topography near the Aldergrove radar site. The dot in the center indicates the radar location. The range ring spacing is 20 km. Also shown in the depiction are the locations of retrieval domains for this case study, enclosed by the inner rectangles

The datasets utilized for this research were collected by the Aldergrove radar on Feb 16, 2002. Several volume scans in sequence revealed two rain bands moving in from the west and the south separately, followed by significant precipitation near the radar site. For this study, Doppler data taken at 3 successive times were considered for the retrieval. The retrieval domains were selected based on the echo extent. The grid spacing was 1000 m in the horizontal and 250 m in the vertical.

3.2 Verification Index

In this research, the accuracy of the LZ wind field is first determined by visual comparisons

To examine how the quality of the retrieval varies spatially, $V_{rad}(retv)$ at each grid point is compared with its radar-observed counterpart $V_{rad}(true)$ by calculating

$$R_{rad} = \frac{|V_{rad}(retv)|}{\sqrt{V_{rad}^2(retv) + V_{rad}^2(true)}} \text{sgn}(V_{rad}(retv) \cdot V_{rad}(true)) \quad (6)$$

The expression $\text{sgn}()$ is used to determine the correctness of the retrieved wind direction. Based on (6), one obtains the following information from which to determine the accuracy of the LZ winds (Liou and Luo 2001).

$R_{rad} = \begin{cases} \sim +1.0: \text{magnitude is seriously overestimated but direction is correct} \\ \sim +0.7: \text{both magnitude and direction are correctly retrieved} \\ \sim 0.0: \text{magnitude is seriously underestimated} \\ \sim -0.7: \text{magnitude is correctly retrieved but direction is wrong} \\ \sim -1.0: \text{magnitude is seriously overestimated and direction is wrong} \end{cases}$

3.3. Retrieval Test

The output of the wind retrieval in the top-left domain is showed in Fig 2. The plot reveals light southwest flow in the southern part of the domain and fairly strong southwest and southerly wind in the north portion.

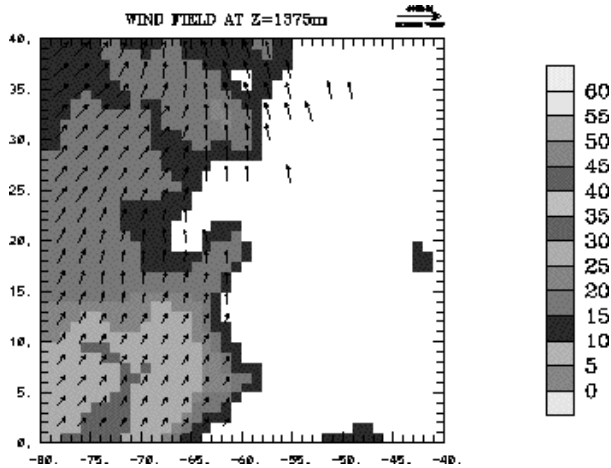


Fig. 2 The retrieved wind field at 16:10 UTC on 16 Feb 2002 from LZ analysis ($Z = 1375\text{m}$). The shaded area denotes the region with radar reflectivity greater than 10 dBZ.

Based on the LZ wind vectors, the retrieved radial wind field is plotted in Fig. 3. When compared with the true radial wind field shown in Fig. 4, it can be seen that the retrieved radial wind agrees reasonably well with the observed one, especially the shape and location of the zero radial wind line.

To study how the quality of the retrieval varies spatially, index R_{rad} , as defined in (6), is calculated and displayed in Fig. 5.

In the plot, the 'bad' retrievals may be identified easily as a very distinct band with R_{rad} values lower than 0.4. The 'good' retrievals are those hatched regions in which the magnitude of R_{rad} ranges from 0.6 to 0.8. By comparison with Fig. 4, it is evident that where the radial component is poorly recovered coincides with where it is also the weaker one. In the regions where the flow is

nearly perpendicular to the radar beam, the radial winds have been obviously underestimated. However, the wind directions are correctly retrieved at most points.

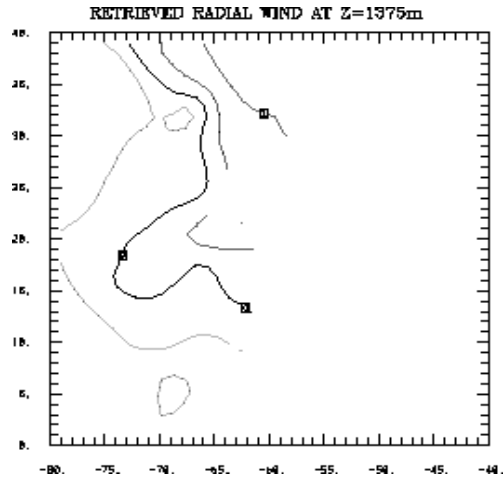


Fig. 3 The retrieved radial wind field at 16:10 UTC on 16 Feb 2002 ($Z = 1375\text{m}$). The contour values have an interval of 0.5 m/s and the zero line is thick.

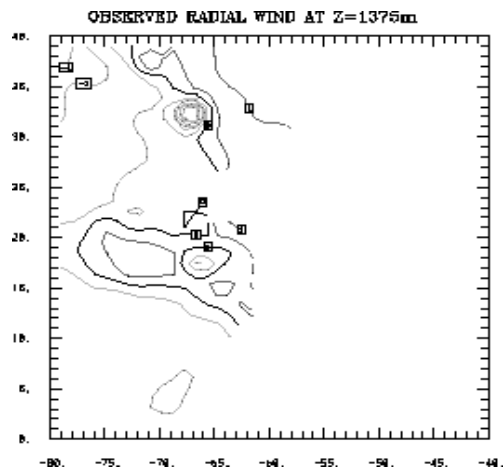


Fig. 4 As in Fig. 3, but for the observed radial wind filed.

3.4 Terrain-modified Flow Features

Fig. 6 gives the retrieved flow structure at the height of 1375 m (ASL) in the lower-left domain. The results indicate that the wind flow split around Vancouver Island, with the east to southeast wind along the Juan de Fuca Strait and south to southeast flow along the Strait of Georgia.

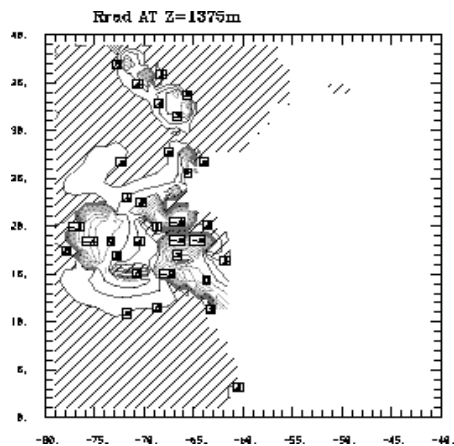


Fig. 5 The distribution of Rrad. The contours range from -1.0 to $+1.0$, with an interval of 0.2 . The hatched region is the region where Rrad range from 0.6 to 0.8 .

A different flow feature was captured in the center domain on 16 Feb 2002, where Doppler data obtained at 18:20, 18:30, and 18:40 UTC were used for the retrieval (Fig. 1).

Results from the retrieval are presented in Fig. 7 for 875 m ASL. There are extensive areas of southerly winds, and a very distinct pattern of light winds in the southwest portion of the domain. The relatively stronger southerly winds in the east domain may be indicative of channeling due to the orographic effects at this level.

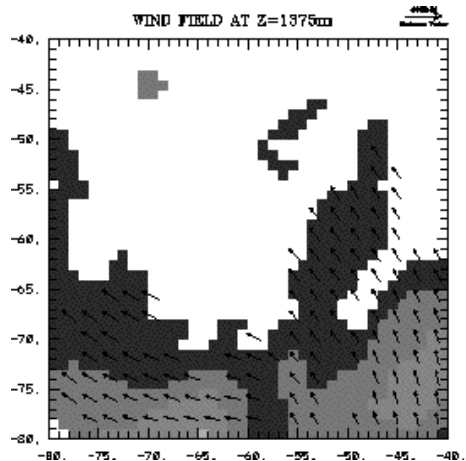


Fig. 6 As in Fig. 2, but for lower-left domain.

4. SUMMARY

In this paper, the LZ SDVR technique was applied to retrieve the 3D wind field over complex terrain from real

single-Doppler data measured on 16 Feb 2002. Without the “correct” flow structure as a reference, the retrieval results were validated against the observed radial component in terms of Rrad indicators.

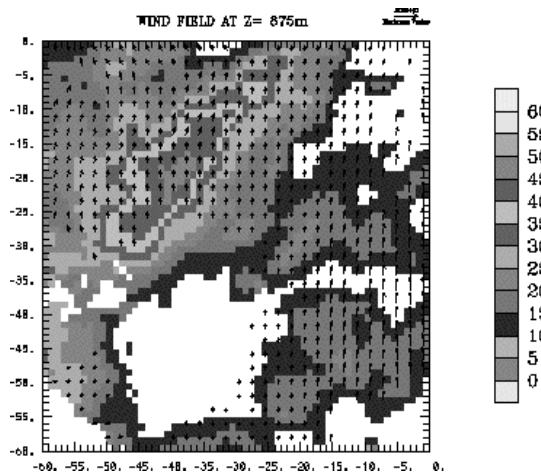


Fig. 7 The retrieved wind field at 18:30 UTC on 16 Feb 2002 from LZ analysis ($Z=875m$).

These preliminary experiment results indicate that:

- The LZ technique was able to successfully retrieve the radial component in most regions.
- Poor retrieval was closely related to weak radial velocity observations.
- In general, the direction of radial velocity was satisfactorily recovered while its magnitude was slightly underestimated.

Future studies will examine more cases and the ‘good’ retrievals indicated by the Rrad index will be assimilated into a mesoscale numerical model. Also, we will use NWP output as a first guess for the wind retrieval.

Reference

Laroche, S., and I. I. Zawadzki, 1994: A variational analysis method for retrieval of three-dimensional wind field from Single-Doppler radar data. *J.Atmos.Sci.*, **51**, 2664-2682

Liou, Y. C., and I. S. Luo, 2001: An investigation of the Moving-Frame Single-Doppler wind retrieval technique using Taiwan area mesoscale experiment low-level data. *J.Appl.Meteor.*, **40**, 1900-1917

Tabary, P., and G. Scialom, 2001: MANDOP analysis over complex orography in the context of MAP experiment. *J.Atmos.Oceanic Technol.*, **18**, 1293-1314